Kontrolované uvolňování

Kamil Záruba

2016-7

Kontrolované uvolňování

- ovlivněním difuze
- ovlivněním botnáním
- změnou chemických aspektů

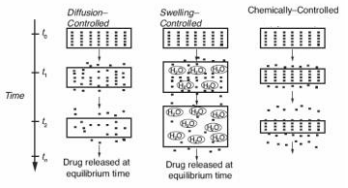

1. Difuzivní uvolňování

- difuzivita API ovlivněna relativní rozpustností v membráně i okolním prostředí; vliv *M*

$$J = -D\left(\frac{dC}{dx}\right)$$

$$\frac{\partial C}{\partial t} = D\left(\frac{\partial^2 C}{\partial x^2}\right)$$

$$D \propto 1/M_w^{1/3}$$

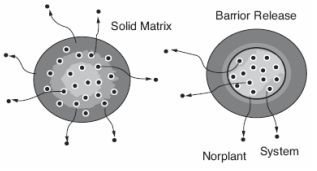

2. Uvolňování bobtnáním matrice

- vysušená forma v kontaktu se tělní tekutinou hydratuje a bobtná; změna velikosti pórů matrice
- hydrogely (60-90% kapaliny, 10-40 % polymeru)

$$\text{Swelling Ratio (SR)} = \frac{\text{Weight of the swollen gel}}{\text{Weight of the dry gel}}$$

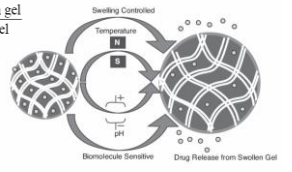

Hydrogely

- hydrogely (60-90% kapaliny, 10-40 % polymeru)
- želatina zesíťovaná glutaraldehydem

- zesíťovaný polyakrylonitril
- poly(vinylalkohol) ve směsi s poly(akrylamid-co-styren)
- 2-hydroxyethylmethakrylát

3. Fyzikálně kontrolované uvolňování

- změna konformace (bio)polymeru (polymerních NP)
  - intermolekulární interakce
  - self-assembly
- změna přitažlivých interakcí na repulsivní (protonizace $NH_2 \rightarrow NH_3^+$; disociace $COOH \rightarrow COO^-$)
- hydrolýza vazeb

Fyzikálně kontrolované uvolňování

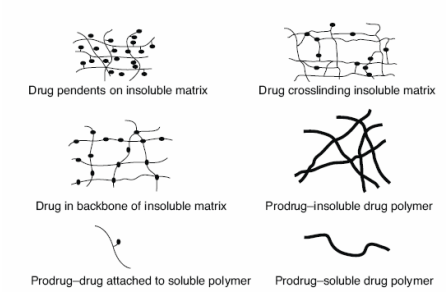

Používané stimuly

- změna teploty
- změna pH
- změna iontové síly
- působení elektromagnetického nebo magnetického pole

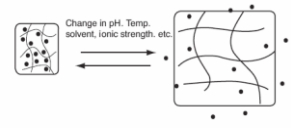

Používané stimuly

Dual-stimuli	pH & magnetic	Fe_3O_4 nanocarrier with peptide mimic polymers
		DOX-tethered Fe3O4 conjugates nanoparticles
		mPEG-b-PMAA-b-PGMA-Fe_3O_4 nanoparticles
		Fe_3O_4-capped MSNs
		MCM-TAA-Fe_3O_4-capped MSNs
	T & redox	EO-PAA-PNIPAAm polymersomes
	Double pH	PPC-Hyd-DOX-DA nanoparticles
		Poly-b-amino ester ketal nanoparticles
	pH & diols	PEG-b-dendritic cholic acid telodendrimers nano-carriers containing boronic acid
	T & magnetic	Pluronic with Fe_3O_4 nanoparticles
	T & enzyme	DNA-capped MSNs
Multi- stimuli	T/pH/redox	PNIPAAm-SS-P(THP-protected HEMA) micelles
	T/pH/magnetic	P(NIPAAm-co-MAA) coated magnetic MSNs
	pH/redox/ magnetic	Fe(II) loaded PMAA crosslinked by N,N-methylene-bisacrylamide and N,N-bis(acryloyl)- cystamine
	T/redox/guest molecule	Vesicles based on hosteguest complex formation between C4AS and MVC12

D. Bennet, S. kim, kap. 8 Polymer Nanoparticles for Smart Drug Delivery, v knize Application of Nanotechnology in Drug Delivery, 2014, InTech Open Access, DOI: 10.5772/58422

Používané faktory

TABLE 32.1 Stimuli-Responsive Smart Polymeric Materials

Type of Stimulus	Responsive Polymer Materials	References
pH	Dendrimers	[71–74]
	Poly(L-lysine) ester	[75]
	Poly(hydroxyproline)	[76]
	Lactose-PEG grafted poly(L-lysine) nanoparticle	[77]
	Poly(L-lysine)-*g*-poly(histidine)	[77]
	Poly(propyl acrylic acid)	[78]
	Poly(ethacrylic acid)	[78]
	Polysilamine	[79]
	Eudragit S-100	[80]
	Eudragit L-100	[81]
	Chitosan	[82]
	PMAA-PEG copolymer	[83]
Ca^{2+}	Alginate	[84]
Mg^{2+}	Chitosan	[85]
Organic solvent	Eudragit S-100	[86]
Temperature[a]	PNIPAAm	[87]
Magnetic field	PNIPAAm hydrogels containing ferromagnetic material PNIPAAm-*co*-acrylamide	[88,89]
Ru^{2+}–Ru^{3+} (redox reaction)	PNIPAAm hydrogels containing tris (2,2′-bipyridyl) ruthenium (II)	[90]
Temperature (sol–gel transition)	Poloxamers	[32,91,92]
	Chitosan-glycerol phosphate-water	[93]

Nanotechnology in Biology and Medicine, Methods, Devices and Applications, T. Vo-Dinh (Ed.), CRC Press, Taylor&Frances Group, London, 2006

Self-assembly (sebeskladba)

- virus tabákové mozaiky

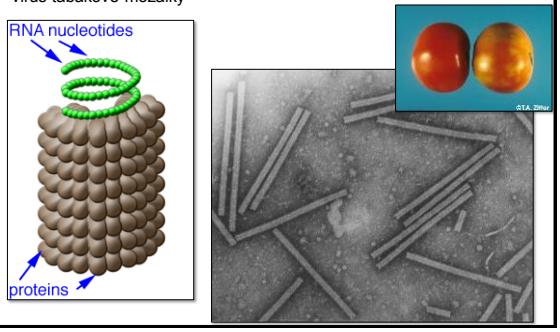

Self-assembly

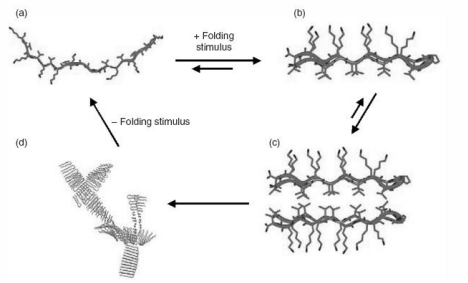

FIGURE 32.3 Triggered folding of a designed peptide (a) led to the formation of a β-hairpin (b), which can self-assemble (c). Ultimately a hydrogel is formed (d), which has a network structure of cross-linked fibrils. Material formation is reversible: simply unfolding the peptides that comprise the assembly dissolves the hydrogel.

Nanotechnology in Biology and Medicine, Methods, Devices and Applications, T. Vo-Dinh (Ed.), CRC Press, Taylor&Frances Group, London, 2006

3.1 Změna teploty

- $\Delta G = \Delta H - T\Delta S$
- enthalpický příspěvek solvatace kompenzován změnou entropie při změně konformace

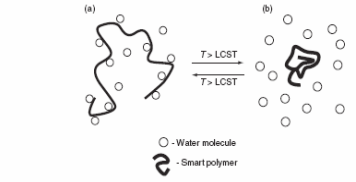

FIGURE 32.6 Schematic of "smart polymer" response with the temperature.

the lower critical solution temperature (LCST)

Nanotechnology in Biology and Medicine. Methods, Devices and Applications. T. Vo-Dinh (Ed.), CRC Press, Taylor&Francis Group, London, 2006

Termoresponsivní hydrogely

- zesíťovaný polymer, 3D síť, reverzibilní změny konformace absorpcí vody a jejím vytěsněním

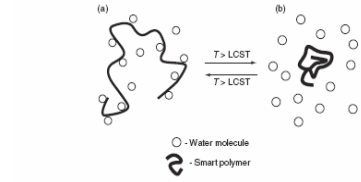

FIGURE 32.6 Schematic of "smart polymer" response with the temperature.

the lower critical solution temperature (LCST)

Nanotechnology in Biology and Medicine. Methods, Devices and Applications. T. Vo-Dinh (Ed.), CRC Press, Taylor&Francis Group, London, 2006

Termoresponsivní hydrogely

- např.:

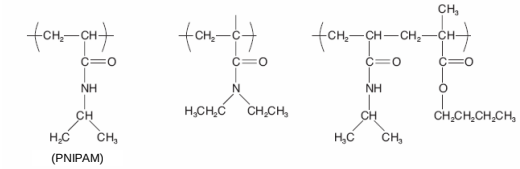

Stimuli Responsive Drug Delivery Systems: Introduction to Application. Bajpai, Shukla, Saini, Tiwari (Eds), iSmithers, UK, 2010

Termoresponsivní hydrogely

- varianta 1

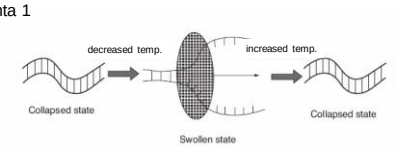

- varianta 2

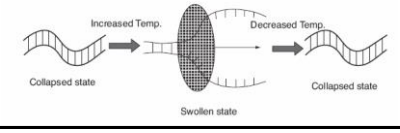

Stimuli Responsive Drug Delivery Systems: Introduction to Application. Bajpai, Shukla, Saini, Tiwari (Eds), iSmithers, UK, 2010

PNIPAM

- poly(*N*-isopropylakrylamid), LCST ≈ 32 °C

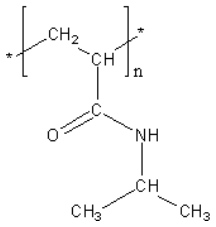

Nanotechnology in Biology and Medicine, Methods, Devices and Applications, T. Vo-Dinh (Ed.), CRC Press, Taylor&Francis Group, London, 2006

PNIPAM

- teplota přechodu (T_{tr}) obecně ovlivněna koncentrací, iontovou silou, povrchově aktivními látkami
- při znalosti fázového diagramu (T_{tr})min = LCST
- u PNIPAM malá závislost T_{tr} na koncentraci

Polymer	Phase transition temperature in aqueous solution
LCST behaviour:	
PNIPAM	30–34 °C
Poly(*N*,*N*-diethylacrylamide)	32–34 °C
Poly(methyl vinyl ether)	37 °C
Poly(*N*-vinylcaprolactam)	30–50 °C (a)
PEO-*b*-PPO (b)	20–85 °C
Poly(GVGVP)	28–30 °C

D. Schmaljohann, Advanced Drug Delivery Reviews 58 (2006) 1655–1670

Aplikace

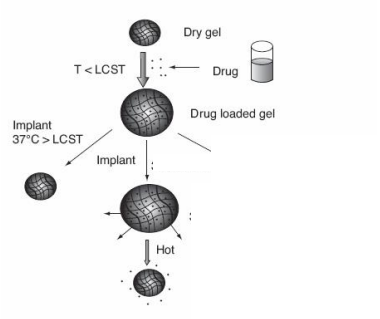

Aplikace (detail)

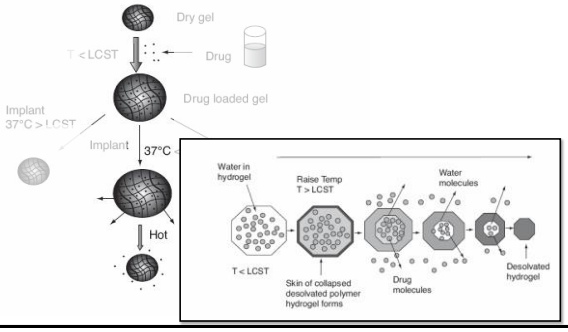

PNIPAM – drug delivery

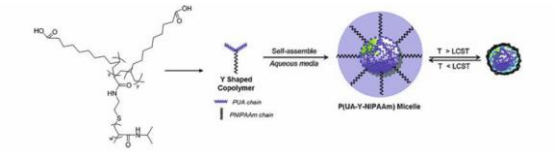

Figure 10.3 Schematic of temperature-sensitive micelles self-assembled in aqueous solutions from Y-shaped copolymers of poly(undecylenic acid) (PUA) and poly(*N*-isopropylacrylamide) (PNIPAAm). Reproduced

- kritická micelární koncentrace 20 mg/ml, LCST = 31 °C
- t > 31 °C → deformace micel, uvolnění léčiva

Nanotechnology in Drug Delivery, M. M. de Villiers, P. Aramwit, G. S. Kwon (Eds.), Springer 2009

PNIPAM – drug delivery

- vznik nanokontejnerů přídavky vody k roztoku poly(2-cinnamoylethyl methakrylát)-blok-poly(N-isopropylakrylamidu) v THF

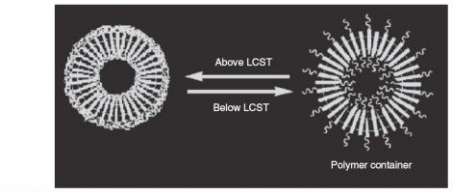

FIGURE 32.7 Schematic illustration of the structural transition behavior of the thermosensitivity of poly(2-cinnamoylethyl methacrylate)-*block*-poly(*N*-isopropylacrylamide), PCEMA–PNIPAM polymer nanocontainers. (Reprinted from Liu, X.-M., Yang Y.-Y., and Leong K.W., *J. Colloid Interface Sci.*, 266, 295, 2003. Copyright (2004) WILEY-VCH Verlag GmbH & Co. KGaA, Weinheim. With permission.)

Nanotechnology in Biology and Medicine, Methods, Devices and Applications, T. Vo-Dinh (Ed.), CRC Press, Taylor&Francis Group, London, 2006

PNIPAM – drug delivery

- orální aplikace inzulinu (hormon slinivky břišní – regulace cukru) a kalcitoninu (hormon štítné žlázy k snižuje hladinu Ca^{2+} v krvi)
- založená na pH indukované hydrolýze polymerních NP – změna struktury PNIPAM teplotou je využita při přípravě NP s imobilizovaným hormonem

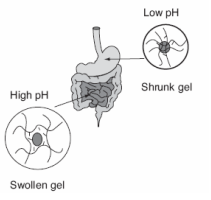

C. Ramkissoon-Ganorkar, F. Liu, M. Baudys, S.W. Kim, Effect of molecular weight and polydispersity on kinetics of dissolution and release from pH/temperature-sensitive polymers, *J. Biomater. Sci., Polym. Ed.* 10 (1999) 1149–1161.

Y.-H. Kim, Y.H. Bae, S.W. Kim, pH/temperature-sensitive polymers for macromolecular drug loading and release, *J. Control. Release* 28 (1994) 143–152.

Další polymery

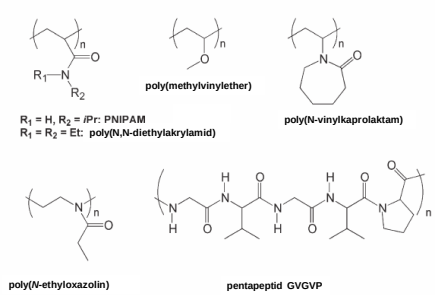

R_1 = H, R_2 = *i*Pr: PNIPAM
R_1 = R_2 = Et: poly(N,N-diethylakrylamid)

D. Schmaljohann, Advanced Drug Delivery Reviews 58 (2006) 1655–1670

Další polymery

- kontrola rychlosti uvolňování obalením PNIPAM vrstvou dalšího polymeru

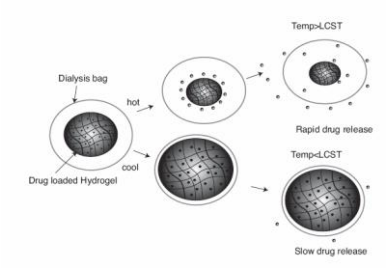

Vliv iontové síly

- vliv změn iontové síly má podobný efekt jako teplota

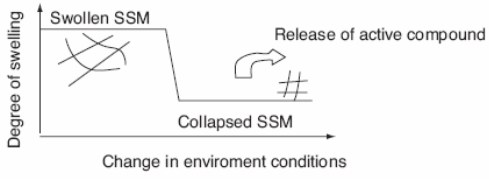

3.2 Změna pH

- konformační změny vyvolané změnou kyselosti okolí
- ionizovatelné polymery s hodnotou pK_a mezi 3 a 10
- karboxylové kyseliny, fosforylové kyseliny, aminy
- monomery: akrylová kyselina, metakrylová kyselina, maleinanhydrid...

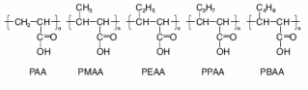

Figure 2.4 Structures of anionic pH-sensitive hydrogels

Změna pH

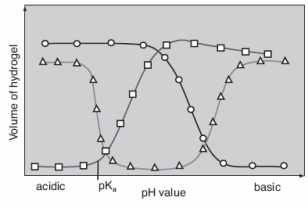

Figure 2.3 Phase transition behaviour of polyelectrolyte hydrogels. Acidic hydrogels (□) are ionised by deprotonation in basic solutions, which have an excess of hydroxyl groups. Basic hydrogels (○) swell in acidic solutions due to the ionisation of their basic groups by deprotonation. Amphiphilic hydrogels (Δ) contain both acidic and basic groups. Therefore, they show two phase transitions

Změna pH

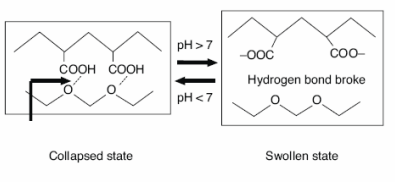

Změna pH

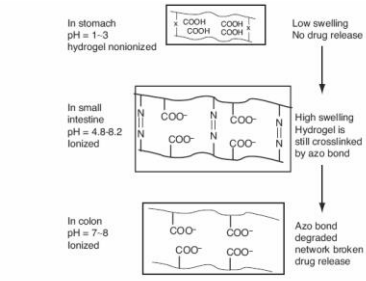

Figure 2.18 Schematic illustration of oral colon-specific drug delivery using biodegradable and pH-sensitive hydrogels. The azoaromatic moieties in the crosslinks are designated by –N=N–

Stimuli Responsive Drug Delivery Systems: Introduction to Application, Bajpai, Shukla, Saini, Tiwari (Eds), Smithers, UK, 2010

Změna pH

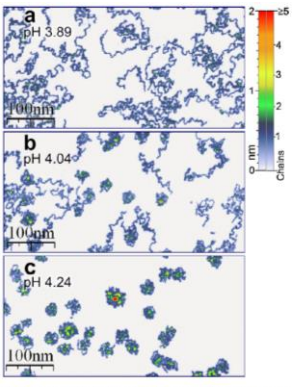

P2VP, poly(2-vinylpyridine);

PE, polyelectrolyte;

Fig. 2. pH-triggered changes in the conformation of single P2VP molecules deposited on the mica substrate from aqueous solutions at different pH. Copyright 2005, the American Chemical Society. Reprinted from Ref. [29] with permission.

Progress in Polymer Science 35 (2010) 174–211

Nevirální transport genů

- kationický polymer vs. anionický oligonukleotid
- polymery s aminoskupinami, poly(ethylenimin), dendrimery, chitosan

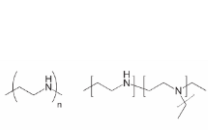

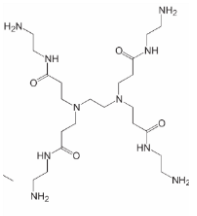

Nevirální transport genů

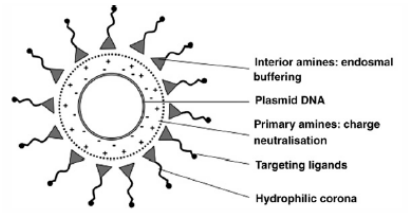

Fig. 5. Self-assembly of PAMAM-PEG-mannose dendritic-linear hybrid polymer with mannose targeting moiety; the system contains primary amines buffering (pK_a=6.9) for complexation of plasmid DNA and tertiary amines (pK_a=3.9) for endosomal buffering, PEG stabilises the polyplex.

D. Schmaljohann, Advanced Drug Delivery Reviews 58 (2006) 1655–1670

Vícevrstevné systémy

- cílený transport ke zvolenému receptoru na povrchu buňky
- hydrolýza některých povrchových skupin
- počátek funkce „skryté“ jednotky

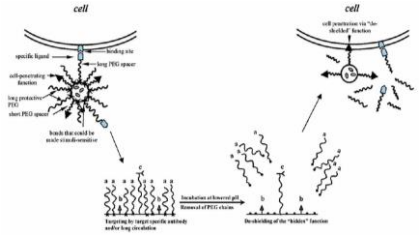

Savant, R. M., J. P.Hurley, et al. (2006). ""SMART" drug delivery systems: doubletargeted pH-responsive pharmaceutical nanocarriers." Bioconjug Chem 17(4): 943–949.

Liposomální formulace

- aniontové liposomy citlivé na pH,
- transport oligonukleotidů po destabilizaci membrány povrchovými skupinami liposomu

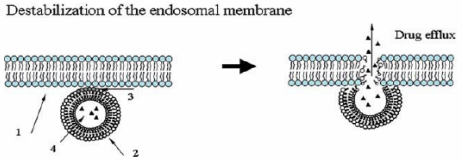

Figure 11.2 Schematics of endosomal drug escape with the use of pH-sensitive liposomes. (1) endosomal membrane; (2) endocytosed liposome; (3) pH-sensitive liposomal component interacting with the endosomal membrane and destabilizing it; (4) liposomal drug

Torchilin, V. P., Zhou, F.,& Huang, L. (1993). pH-Sensitive liposomes. J Liposome Res, 3, 201–255.

Micelární formulace

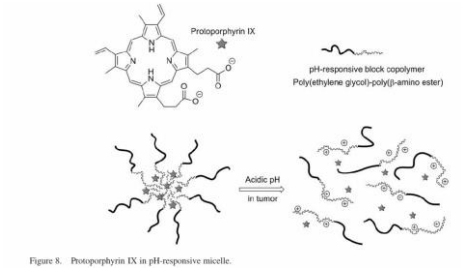

Figure 8. Protoporphyrin IX in pH-responsive micelle.

Kim, K.; Koo, H.; Lee, H.; Lee, S.; Min, K.H.; Kim, M.S.; Lee, D.S.; Choi, Y.; Kwon, I.C.; Jeong, S.Y. *Chem. Commun.* 2010, 46 (31), 5668–5670.

Porézní křemičité nanočástice

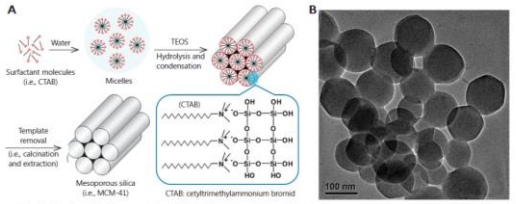

Figure 1 Synthesis scheme for the preparation of MSNs (A) and transmission electron microscopy (TEM) images of MCM-41 (B). (**Figure 1A** is adapted from Ref. 22 with permission of The Royal Society of Chemistry).

Cancer Biol Med 2014;11:34-43

Porézní křemičité nanočástice

- multivrstva polyelektrolytu (poly(allylamin hydrochlorid) a poly(styrenesulfonát) sodný) se v kys. prostředí rozpadá

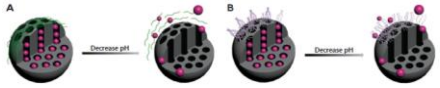

- protonizace dusíku heterocyklu snižuje afinitu k cyklodextrinu

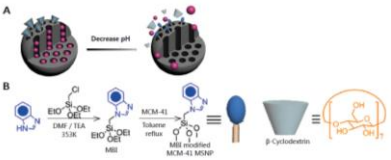

Cancer Biol Med 2014;11:34-43

Porézní křemičité nanočástice

- multivrstva polyelektrolytu (poly(allylamin hydrochlorid) a poly(styrenesulfonát) sodný) se v kys. prostředí rozpadá

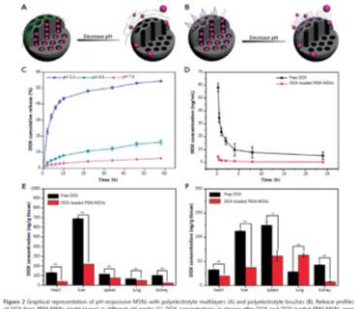

Cancer Biol Med 2014;11:34-43

3.3 Kombinace T a pH

- transport do tumoru s nízkým pH
- při pH < 6,6 je LSCT < 37°C

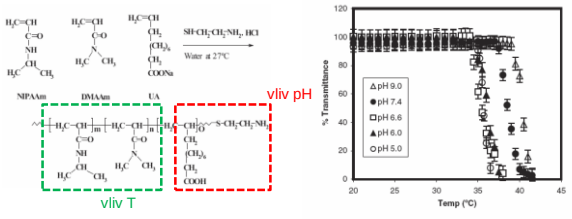

Figure 1. Plot of transmittance of Polymer II solutions as a function of temperature at varying pH at 500 nm.

Soppimath et al., Adv. Mater. 2005, 17 , 318–323

3.4 Oxidace

- vedle EPR faktoru charakterizují tumory také speciální makrofágy uvolňující oxidující molekuly
- kopolymer ABA
- A = PEG – hydrofilní, brání adsorpci proteinů, málo toxický
- B = poly(propylensulfid) – hydrofobní, oxidovatelný

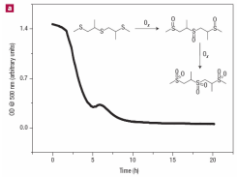

Soppimath et al., Adv. Mater. 2005, 17 , 318–323

Oxidace

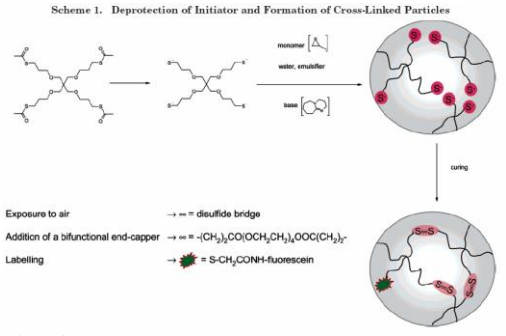

Rehor et al. Langmuir 2005, 21, 411-417

4. Chemické stimuly

- vliv přítomnosti iontů

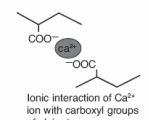

Ionic interaction of Ca^{2+} ion with carboxyl groups of alginate

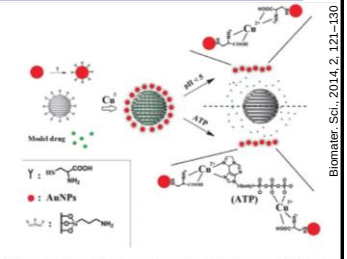

Biomater. Sci., 2014, 2, 121–130

Scheme 1 Schematic representation of the AuNPs-capped-MSN based drug delivery system. The controlled-release mechanism of the system is based on forming and breaking of ligand bond between the AuNPs caps, Cu^{2+} and the MSN hosts. The scheme is presented by (A) MSN functionalization, (B) AuNP functionalization, (C) AuNP capping of MSNs, (D) AuNP displacement by pH mechanism and (E) AuNP displacement by interaction with ATP.

4. Chemické stimuly

- vliv přítomnosti proteinů

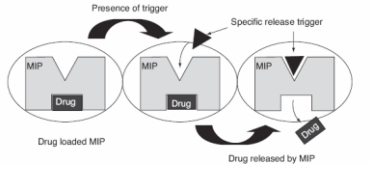

Chemické stimuly

- duální stimul
- hydrogel na bázi PEG-oligopeptidu a dextranu
- k hydrolýze nutná přítomnost nukleasy i dextranasy

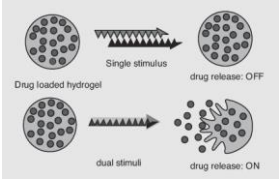

Chemické stimuly

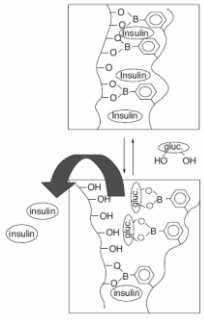

Sledování kinetiky uvolňování z NP

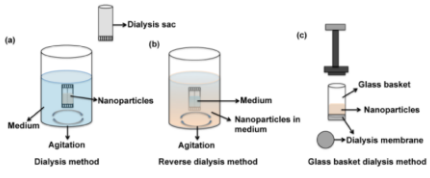

Fig. 1.
Schematic representation of dialysis methods. (a) dialysis sac method, the nanoparticulate systems are placed inside the dialysis sacs; (b) reverse dialysis sac method, the nanoparticulate systems are added to the medium outside the dialysis sacs and the inside medium is analyzed for released drug at different time intervals; and (c) glass basket dialysis method, a glass cylinder with its bottom sealed by a dialysis membrane is used.

Sledování kinetiky uvolňování z NP

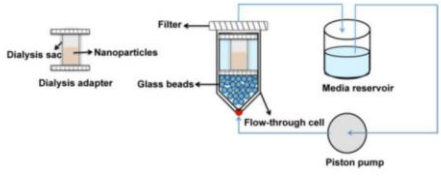

Fig. 2.
Schematic representation of dialysis adapter based USP 4 method in a closed loop configuration. Glass beads are added in the flow through cell to facilitate laminar flow of the media throughout the cell.

Sledování kinetiky uvolňování z NP

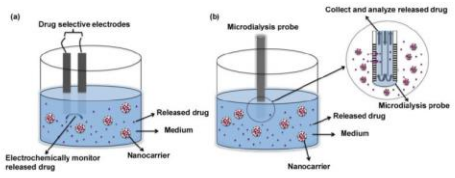

Fig. 3.
Schematic representation of (a) drug-selective electrode based methods, drug release is monitored electrochemically; and (b) microdialysis based methods, where a microdialysis tube is used to monitor drug release profiles. The microdialysis tube is constructed as a concentric tube, where the perfusion fluid enters through an inner tube, and flows back between the inner tube and the outer dialysis membrane.

Sledování kinetiky uvolňování z NP

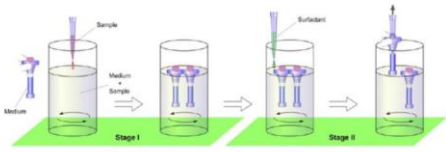

Fig. 4.
Schematic representation of a two stage reverse dialysis sac method (reprinted with permission) (18). Stage 1: liposomes were added to the exterior medium and samples were taken from the interior of alternative dialysis tubes; Stage 2: surfactant (Triton X-100) was added to the exterior medium and samples were taken from alternative dialysis tubes. At least two tubes are used to allow equilibration prior to the next sampling time.

Kinetické modely uvolňování z NP

Mathematical models used to describe drug dissolution curves

Zero order	$Q_t = Q_0 + K_0 t$
First order	$\ln Q_t = \ln Q_0 + K_1 t$
Second order	$Q_t/Q_\infty(Q_\infty - Q_t)K_2 t$
Hixson–Crowell	$Q_0^{1/3} - Q_t^{1/3} = K_s t$
Weibull	$\log[-\ln(1-(Q_t/Q_\infty))] = b \times \log t - \log a$
Higuchi	$Q_t = K_H\sqrt{t}$
Baker–Lonsdale	$(3/2)[1-(-1(Q_t/Q_\infty))^{2/3}] - (Q_t/Q_\infty) = Kt$
Korsmeyer–Peppas	$Q_t/Q_\infty = K_k t^n$
Quadratic	$Q_t = 100(K_1 t^2 + K_2 t)$
Logistic	$Q_t = A/[1+e^{-K(t-y)}]$
Gompertz	$Q_t = A\ e^{-e-K(t-y)}$
Hopfenberg	$Q_t/Q_\infty = 1-[1-k_0 t/C_0 a_0]^n$

P. Costa et al. Eur. J. Pharm. Sci. 2001, 13, 123-133

Modelování – iterační výpočet

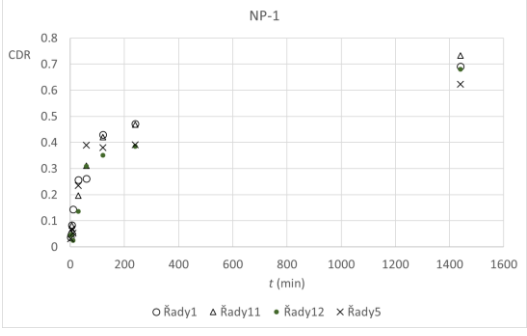

Modelování – iterační výpočet

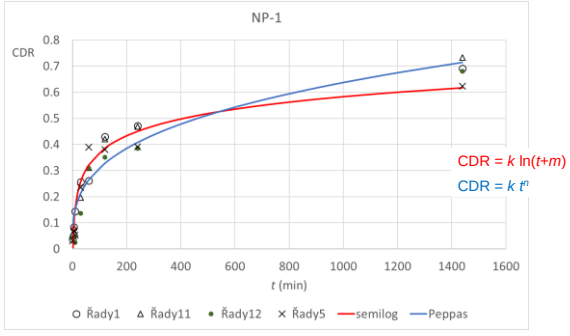

Modelování – iterační výpočet